

CHAPTER IV

RESULTS AND DISCUSSION

4.1 α -Chitin whisker morphology

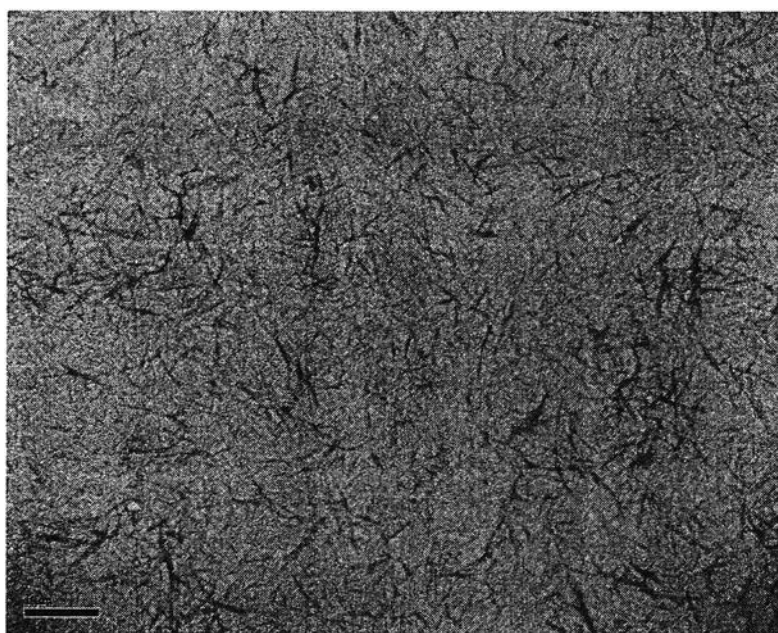


Figure 4.1 TEM image of α -chitin whisker at 10000x.

The morphology of the diluted suspension of α -chitin whisker is shown in Fig. 4.1. The TEM image shows a colloidal behavior due to the repulsion of the positive charge (NH_3^+) on the suspension surface. The size distribution of the chitin whisker is shown in Figs. 4.2 and 4.3. The length of the chitin whisker ranged from 370 to 860 nm, while the width ranged from 20 to 80 nm. Moreover, the average length and width of the whiskers were 517.53 and 27.93 nm, respectively, compared to our previous study (Sriupayo, J. *et al.*, 2005) which presented the average length and width of the chitin fragments at 417 and 33 nm, respectively. There was no significant difference in the size

of the chitin whiskers, so this evaluation suggests that this method was suitable for chitin whisker preparation.

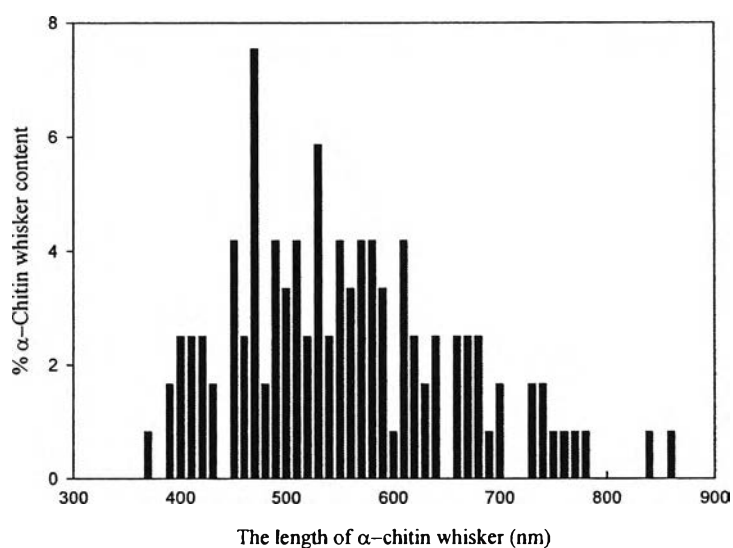


Figure 4.2 Histogram of the length distribution of α -chitin whisker.

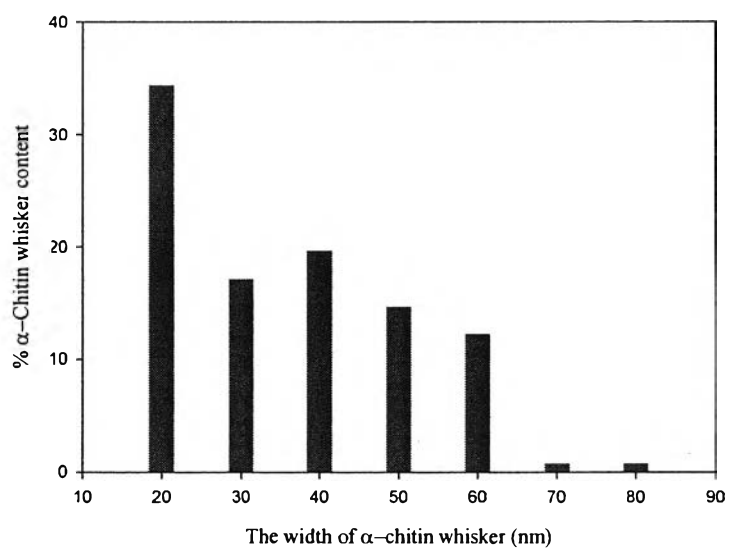


Figure 4.3 Histogram of the width distribution of α -chitin whisker.

4.2 Appearance of films

β -Chitin film and α -chitin whisker-reinforced β -chitin films were formed by using solvent casting technique. Chitin gel was easily dissolved in concentrated formic acid whereas chitin powder was rarely dissolved in that solvent even in other common solvents. The preparation of nanocomposite film, β -chitin was matrix and α -chitin whisker was reinforced filler, can be highly produced the good dispersed film. Moreover, the pure chitin film was transparent whereas chitin nanocomposite films were more translucent as the increase with the α -chitin whisker content. Interestingly, all of as-prepared films were flexible unlike the nature of chitin. The thickness of all of films was presented into table 4.1, for the thickness result showed that the increase of α -chitin whisker content trended to increase the thickness of films.

Table 4.1 Thickness of pure β -chitin film and chitin nanocomposite films

Film	Thickness (μm)
1% β -Chitin (pure)	24.32 ± 3.92
1% β -Chitin + 0.25% α -Chitin whisker	24.42 ± 4.29
1% β -Chitin + 0.5% α -Chitin whisker	24.79 ± 2.14
1% β -Chitin + 0.75% α -Chitin whisker	25.69 ± 1.48
1% β -Chitin + 1% α -Chitin whisker	31.31 ± 2.64
1% β -Chitin + 1.5% α -Chitin whisker	35.40 ± 2.33
1% β -Chitin + 2% α -Chitin whisker	45.88 ± 2.94

4.2 Mechanical Properties

4.3.1 Tensile Strength

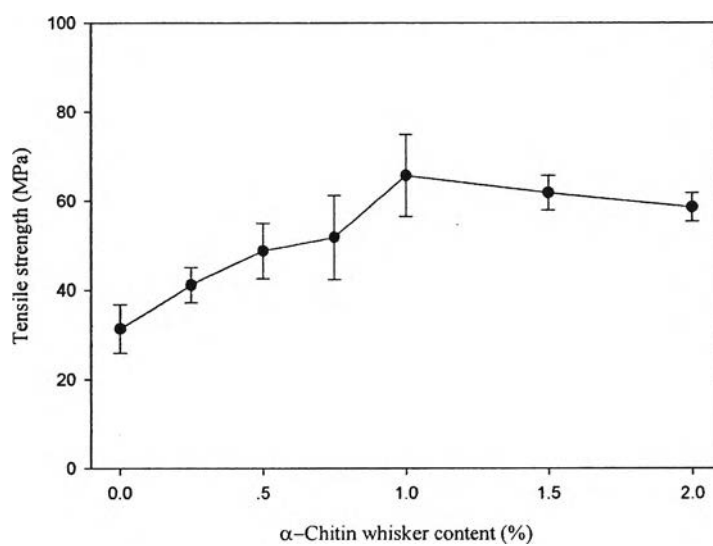


Figure 4.4 Tensile strength of pure β -chitin film and α -chitin whisker-reinforced β -chitin films in various content of whisker.

4.3.2 Percentage of strain at break

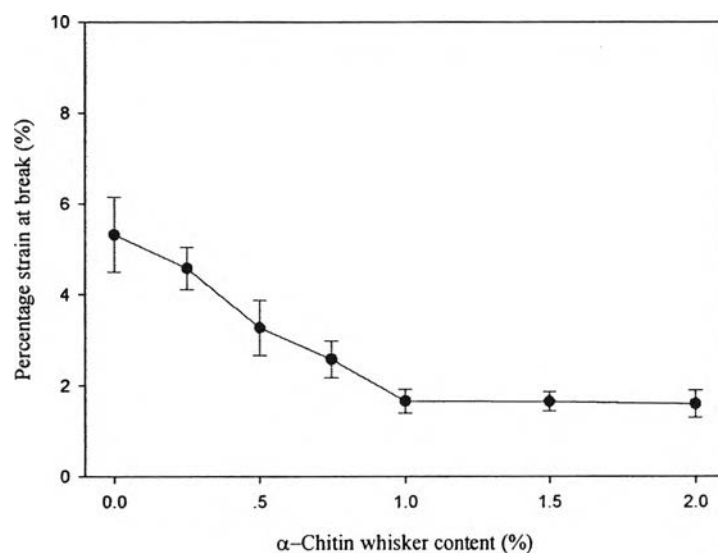


Figure 4.5 Percentage strain at break of pure β -chitin film and α -chitin whisker-reinforced β -chitin films in various content of whisker.

4.3.3 Tensile modulus

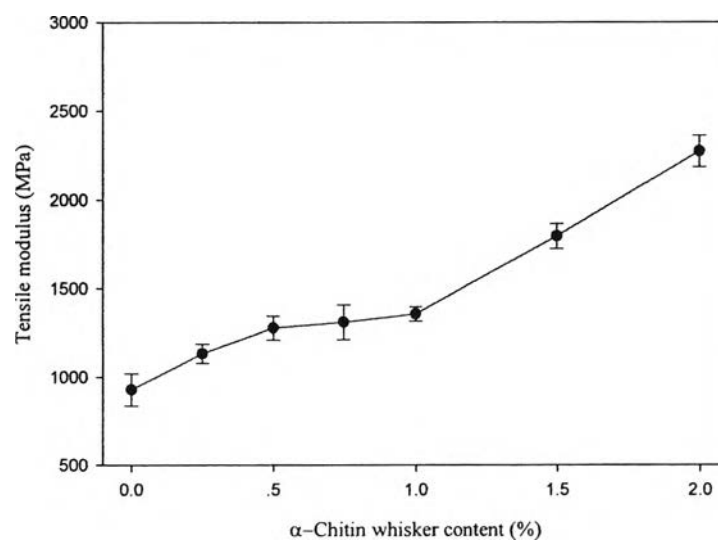


Figure 4.6 Tensile modulus of pure β -chitin film and α -chitin whisker-reinforced β -chitin films in various content of whisker.

Tensile strength, tensile modulus and percentage of strain at break of pure chitin film and α -chitin whisker-reinforced chitin films were investigated. Fig 4.4 show tensile strength of pure chitin film and α -chitin whisker-reinforced chitin films in the range of 0.25-2% whisker content, the result found that the increasing of α -chitin whisker content trend to higher tensile strength. Initially from pure chitin film, tensile strength of pure chitin film was 31.39 ± 5.46 . For 0.25, 0.5, 0.75, 1, 1.5 and 2% α -chitin whisker were 41.12 ± 3.88 , 48.73 ± 6.22 , 51.76 ± 9.46 , 65.68 ± 9.20 , 61.80 ± 3.90 and 58.58 ± 3.17 , respectively. For the value of tensile strength found that it increased continuously to reach the maximum point at 1% α -chitin whisker contained film and it gradually decreased after the α -chitin whisker content was over 1% w/v. On the other of the tensile strength, the percentage of strain at break shows in fig 4.5 decreased steadily from that of the pure chitin film (i.e. $5.32 \pm 0.83\%$) with increasing whisker content. The percentage of strain of nanocomposite films also showed 4.58 ± 0.47 , 3.26 ± 0.60 , 2.58 ± 0.40 , 1.66 ± 0.26 , 1.64 ± 0.21 and 1.59 ± 0.30 for 0.25, 0.5, 0.75, 1, 1.5 and 2% α -chitin whisker, respectively, whereas the tensile modulus of nanocomposite films fig 4.6 trend to follow in the same way of tensile strength, their modulus initially increased from 928.76 ± 90.38 MPa of pure chitin film to 1132.51 ± 53.56 , 1277.87 ± 68.35 , 1310.10 ± 98.08 , 1356.16 ± 40.68 , 1794.46 ± 69.94 and 2272.43 ± 88.78 MPa of 0.25, 0.5, 0.75, 1, 1.5 and 2% α -chitin whisker, respectively. The increase in the tensile strength of the nanocomposite films might be due to the hydrogen bonding between the α -chitin whisker reinforcing filler and the β -chitin matrix. This interaction affects the rigidity of the nanocomposite films, causing the tensile modulus to also increase whereas the percentage of strain at break decreases.

In comparing the tensile strength of the β -chitin film with other studies, the present study finds that it is greater than in the report of Peesan, M. *et al.* (2003) who reported 5.1 MPa. That different result might be caused by the different route of β -chitin film preparation.

4.3 Thermal Property

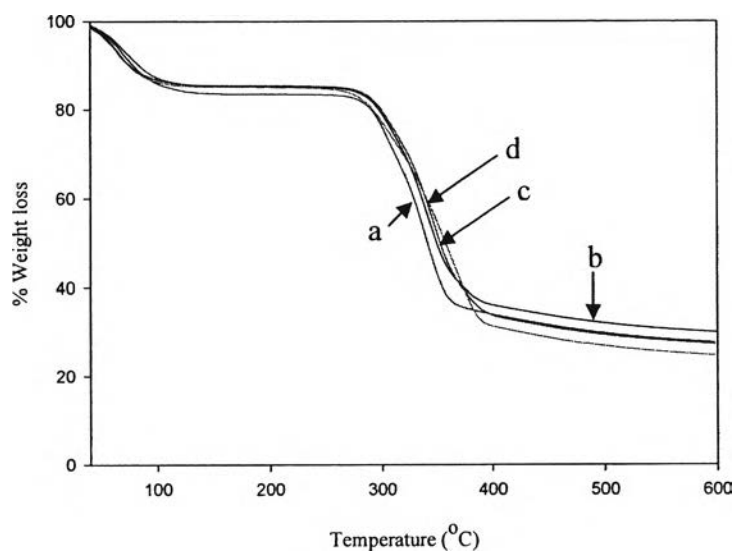


Figure 4.7 Thermogravimetric analysis of pure β -chitin film (a), α -chitin whisker-reinforced β -chitin films in 0.25% (b), 0.5% (c) and 0.75% (d).

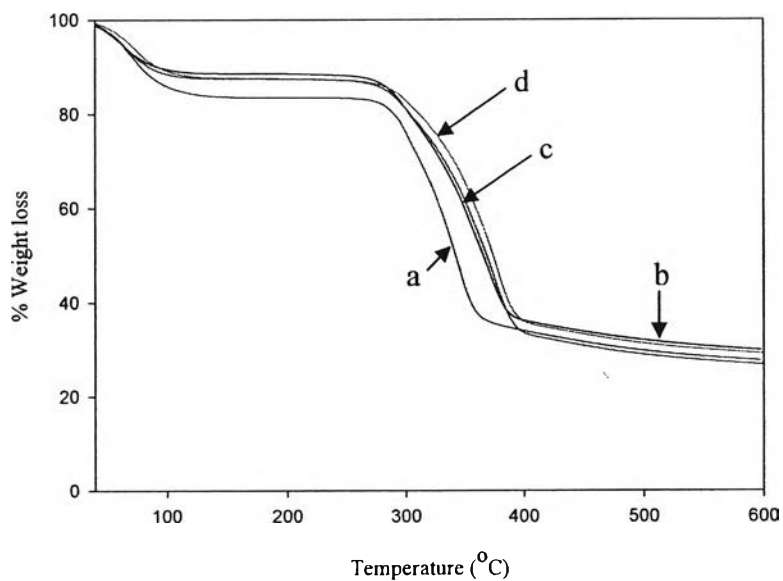


Figure 4.8 Thermogravimetric analysis of pure β -chitin film (a), α -chitin whisker-reinforced β -chitin films in 1% (b), 1.5% (c) and 2% (d).

The thermal stability of the films was evaluated by TGA; the TGA thermograms of pure β -chitin and α -chitin whisker-reinforced β -chitin films are shown in Fig. 4.7 and 4.8. The thermal degradation of the films is shown by two steps. Firstly, all films had an initial weight loss at about 60-80°C, due to the loss of moisture upon heating. Secondly, the decomposition temperature (T_d) was identified starting with pure chitin (341°C), which nearly equals that reported by Peesan, M. *et al.* (2003), who also investigated the decomposition temperature of β -chitin films, resulting about 349°C. In the cases of the 0.25%, 0.5%, 0.75%, 1%, 1.5% and 2% α -chitin whisker contained nanocomposite films; the decomposition temperature was 343, 346, 366, 370, 376 and 377°C respectively, which explains the degradation of the acetylglucosamine main chain structure (Tanodekaew, S. *et al.*, 2004). The T_d of the nanocomposite films slightly increased with the increase in the content of α -chitin whisker. Compared to the effect of α -chitin whisker reinforced chitosan and poly(vinyl alcohol), it was found that α -chitin whisker slightly improved the thermal stability of their nanocomposite films (Sriupayo, J. *et al.*, 2005). In the present study, the results suggest that the presence of α -chitin whisker might improve the thermal stability of the nanocomposite films because the α -chitin whisker mainly provides the interaction with β -chitin matrix.

4.4 FTIR Study

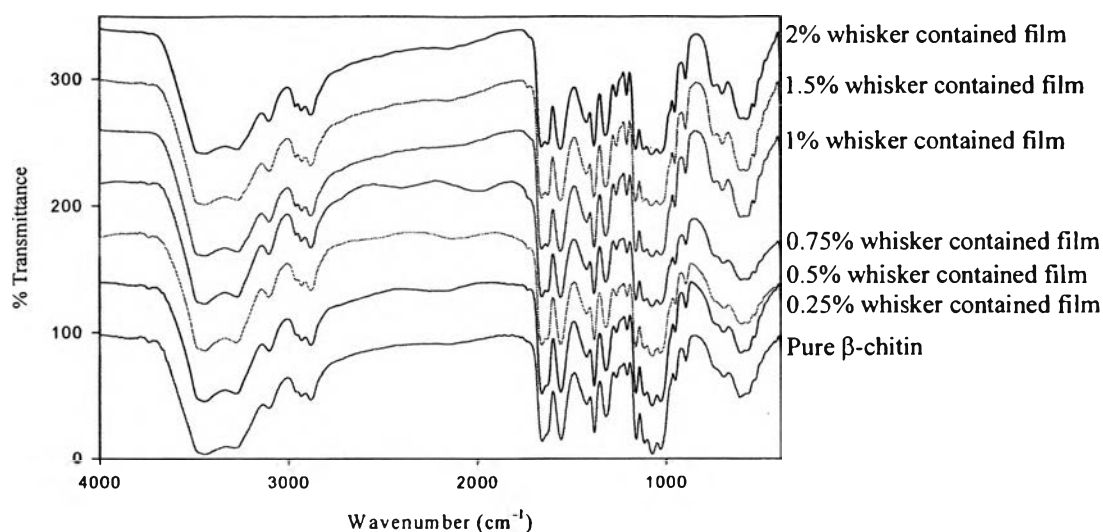


Figure 4.9 FTIR results of pure β -chitin film and α -chitin whisker-reinforced β -chitin films in various content of whisker.

Fig. 4.9 shows the FTIR spectra of the pure chitin and nanocomposite films. The important peaks of chitin appeared at about $3200\text{--}3500\text{ cm}^{-1}$, which corresponds to NH- and OH-stretching. At 1660 and 1558 cm^{-1} , C=O stretching as amide I and amide II, respectively, also appears. The different wavenumbers of amide I and II could be due to the differences of interaction effects. Amide I was ascribed to the effect of the intermolecular hydrogen bonding of C=O---N-H and of the intramolecular hydrogen bonding of C=O---OHCH₂ (Lavall, R.L. *et al.*, 2006). In the case of amide II, the band at 1558 cm^{-1} arose from the deformation of the intramolecular hydrogen bonding, N—H bond in the plane of the CONH group (Nge, T.T. *et al.*, 2003). The degree of deacetylation (%DD) of the films could be calculated from the FTIR spectra using the method of Khan, T.A. *et al.* (2002). The %DD of the film ranged from about 15-30%, compared with the chitin powder (14%). After the film was processed by solvent casting, the %DD changed slightly.

In addition, from the FTIR spectra, the characteristic peaks of the nanocomposite films are unaffected, compared to the β -chitin film. No peaks shift and no new peaks are observed. This investigation, then, may possibly explain that the interaction of α -chitin whisker and β -chitin matrix is only a physical interaction via hydrogen bonding.

4.5 Water Adsorption Ability

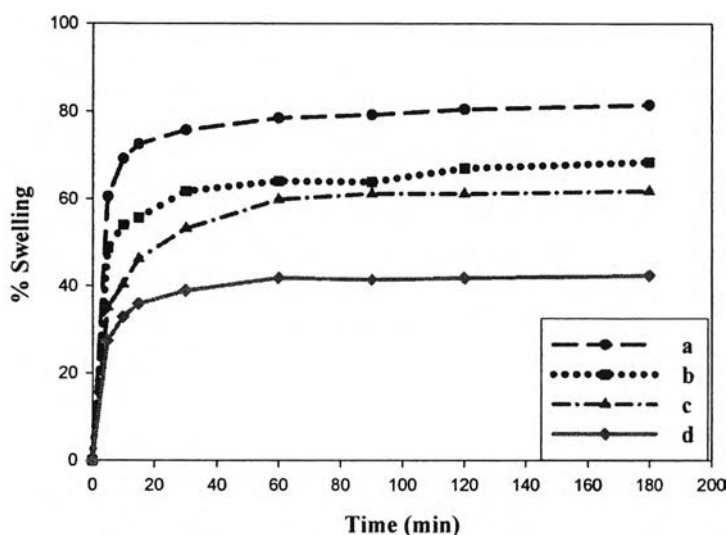


Figure 4.10 Percentage of swelling of pure β -chitin film (a), 0.5% α -chitin whisker nanocomposite film (b), 1% α -chitin whisker nanocomposite film (c) and 2% α -chitin whisker nanocomposite film (d).

The percentage of swelling of the films was plotted as a function of the immersion time, as shown in Fig. 4.10. All films sharply increased with initial immersion time up to 10 min. After that, the percentage of swelling gradually increased to reach an equilibrium point after an immersion time of about 60 min. The nanocomposite films provided a lower percentage of swelling than the pure chitin film. Swelling value reached the highest point with the β -chitin film (81.46%), and

continuously decreased with the increase in the content of α -chitin whisker, including 68.43%, 61.82%, and 42.36% of 0.5%, 1% and 2% α -chitin whisker films, respectively. The percentage of swelling of the β -chitin film was higher than the α -chitin film, from the report of Park, K.E. *et al.* (2006) as about 62.5%, an effect of the strong hydrogen bonding of α -chitin. The swelling behavior of the films in this study suggests that it is dependent on the presence of α -chitin whisker, which is inversely proportional to the degree of swelling. This might come from the fact that the α -chitin whisker acts as a water barrier to obstruct water diffusion.

4.6 *In Vitro* Biodegradability

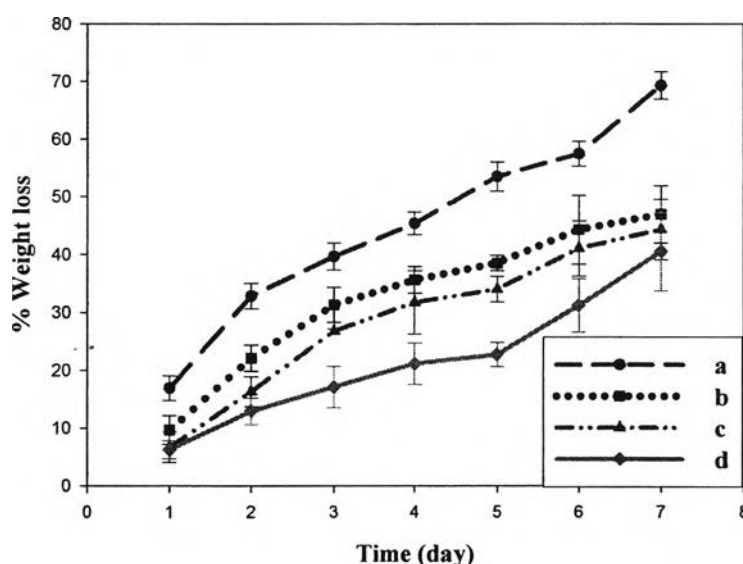


Figure 4.11 Percentage of weight loss after enzymatic hydrolysis of pure β -chitin film (a), 0.5% α -chitin whisker nanocomposite film (b), 1% α -chitin whisker nanocomposite film (c) and 2% α -chitin whisker nanocomposite film (d).

Chitin is known to be a biopolymer that can be degraded in a suitable enzyme. Normally, chitin displays no discernible degradation in a neutral media at room

temperature (Tomihata, K. *et al.*, 1997). Lysozyme from hen egg white could be used to degrade chitin to oligochitin and later to N-acetylglucosamine (Cho, Y.W. *et al.*, 1999). In nature, the chitin conformation may occur in α -, β -, and γ -chitin. The rates by which these forms of chitin are hydrolyzed by lysozyme are different and because of their crystallinity (Sujins, J. *et al.*, 1973). Additionally, there are a lot of things that affect the rate of degradation; like crystallinity, molecular weight and morphological structure (Noh, H.K. *et al.*, 2006). In the case of β -chitin, it was reported to be degraded in lysozyme in PBS for one week and a large content of β -chitin in the film could enhance the amount of weight loss of the film after enzymatic hydrolysis (Lee, Y.M. *et al.*, 2003). On the other hand, the chitin fibers were also investigated to determine their biodegradability in lysozyme. Chitin microfibers and chitin nanofibers were compared for the ability of enzymatic hydrolysis. The results showed that the rate of degradation of the chitin nanofibers was significantly higher than the chitin microfibers. When comparing the rates of degradation between chitin and chitosan, the rate trends to decrease with an increase of the degree of deacetylation. That means that chitosan enhances the rate of biodegradability (Tomihata, K. *et al.*, 1997).

To evaluate the biodegradability of the films in the present study, the films were incubated in lysozyme containing PBS at 37°C for 7 days. Fig. 4.11 shows the percentage of weight loss of films after enzymatic hydrolysis. The obtained results show that most of the films could be degraded by enzymatic hydrolysis within 7 days and the pure chitin film was degraded easier than nanocomposites films. The weight reduction of the films was probably due to the loss of the β -chitin matrix on the surface and the weight loss of the films decreased as the α -chitin whisker content increased. The results might be explained in that the resulting α -chitin whiskers act as a barrier to prevent the diffusion of lysozyme inside the films.

To confirm the enzymatic hydrolysis, the microarchitecture of the films was analyzed by SEM. The results show that the surface morphology of films after enzymatic hydrolysis was rougher than the original films, as shown in Fig. 4.12.

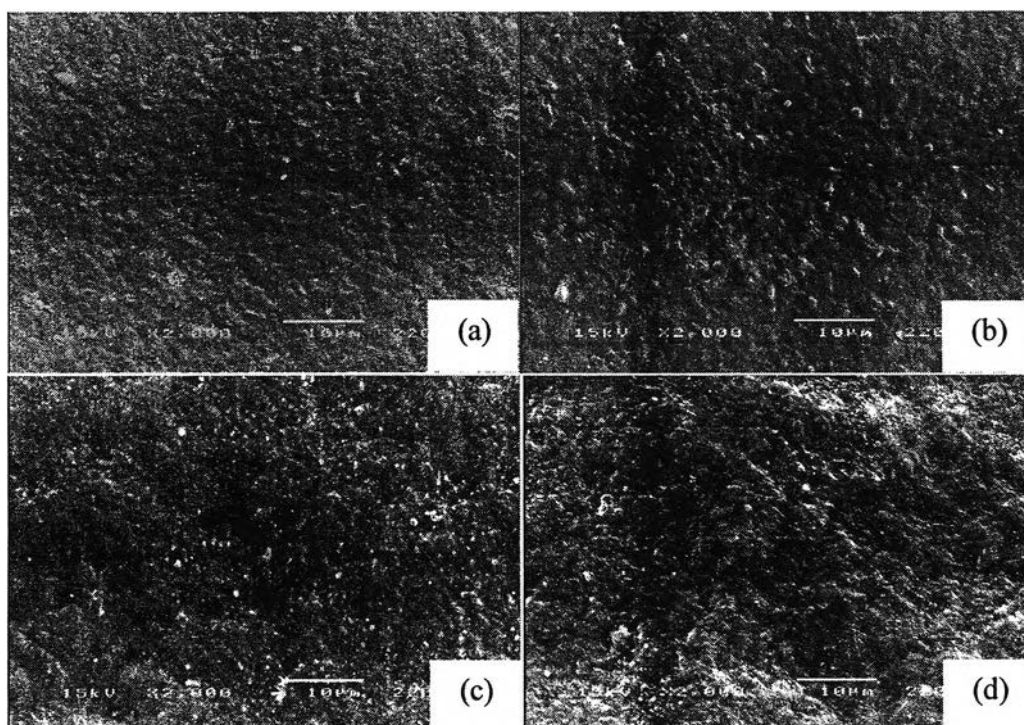


Figure 4.12 The surface morphology of films investigated by SEM to display the effect of biodegradability of film under enzymatic hydrolysis, (a) and (b) show the surfaces of pure β -chitin film before and after enzymatic hydrolysis for 7 days, respectively, (c) and (d) show the surface of 2% w/v α -chitin whisker nanocomposite film before and after enzymatic hydrolysis for 7 days, respectively.

4.7 Oxygen Permeability

Oxygen permeation across the chitin and nanocomposite films was studied by measuring the permeance at which oxygen passes through the mounted films in the gas chamber. According to ASTM D1434, the oxygen permeance and oxygen permeability can be calculated by the following equations:

$$\text{Oxygen permeance, } P = 1.49 \times 10^7 / KN \quad (4)$$

$$\text{Oxygen permeability, } \underline{P} = G \times 5.16435 \times \text{thickness (mm)} \quad (5)$$

where K is absolute temperature and N is the slope of graph (mm/sec).

Table 4.2 The oxygen permeability rate and permeability of β -chitin film and chitin nanocomposite films

Type of films	P (Permeance) mol/m ² .s.Pa ($\times 10^{18}$)	<u>P</u> (Permeability) mol/m.s.Pa ($\times 10^{18}$)
1% β -Chitin film	554.68	54.283
1% β -Chitin + 0.5% α -Chitin whisker	146.254	12.236
1% β -Chitin + 1% α -Chitin whisker	38.838	5.305
1% β -Chitin + 2% α -Chitin whisker	18.186	4.701

Table 4.2 presents the oxygen permeance and oxygen permeability through the chitin and the nanocomposite films. Observation shows that the chitin film possesses the highest permeance and permeability of oxygen, whereas the chitin nanocomposite films show a lower oxygen permeance with an increase in chitin whisker content. In only the 0.5% chitin whisker added to the chitin matrix was there as much of an effect on the oxygen permeance. It increased from 554×10^{-18} to 146×10^{-18} mol/m².s.Pa. This result suggests that the addition of chitin whisker obstructs the permeability of oxygen through the films, resulting in the chitin whisker acting as a gas barrier.

4.8 X-ray Diffraction

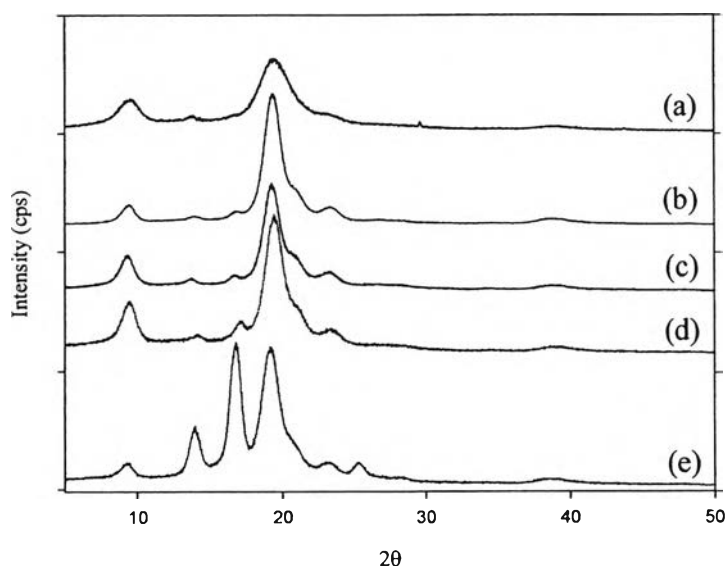


Figure 4.13 The WAXD patterns of chitin film (a), 0.5% α -chitin whisker contained film (b), 1% α -chitin whisker contained film (c), 2% α -chitin whisker contained film (d) and α -chitin whisker (e).

The crystalline structure of the α -chitin whisker, chitin films and chitin nanocomposite films were observed by WAXD. Fig. 4.13 shows the characteristic diffraction of the α -chitin whisker (a), the chitin nanocomposite films (b, c, and d) and the β -chitin film (e). The β -chitin films showed diffraction peak 2θ at 9.5° and 19.4° , the chitin whisker showed diffraction peak 2θ at 9.4° , 14° , 16.8° , 19.2° and 21.1° , while the diffraction peak 2θ of chitin nanocomposite films appeared at 9.3° , 17° , 19.3° and 21° . Therefore, the chitin whisker does not affect the crystallinity of the chitin matrix because the WAXD patterns of the nanocomposite films continue to show the crystalline characteristic of the chitin matrix.

Yen, M.-T. and Mau, J.-L. (2007) found that the diffraction peaks of β -chitin was 9.1° and 20.3° . On the other hand, the diffraction peaks of α -chitin were 9.6° , 19.6° ,

and 23.7° . Jang, M.-K. *et al.* (2004) found that α -chitin was observed to have four diffraction angles at 9.6° , 19.6° , 21.1° , and 23.7° . Also, β -chitin was observed to have two diffraction angles at 9.1° and 20.3° . The observation of the WAXD pattern of chitin was reported by Ren, L. and Tokura, S. (1994) who interpreted the diffraction peaks of β -chitin at 8.5° and 19.98° , which corresponds to the (010), and (020) and (110) planes, respectively.

4.10 Cytotoxicity Test by Indirect Method (MTT Assay)

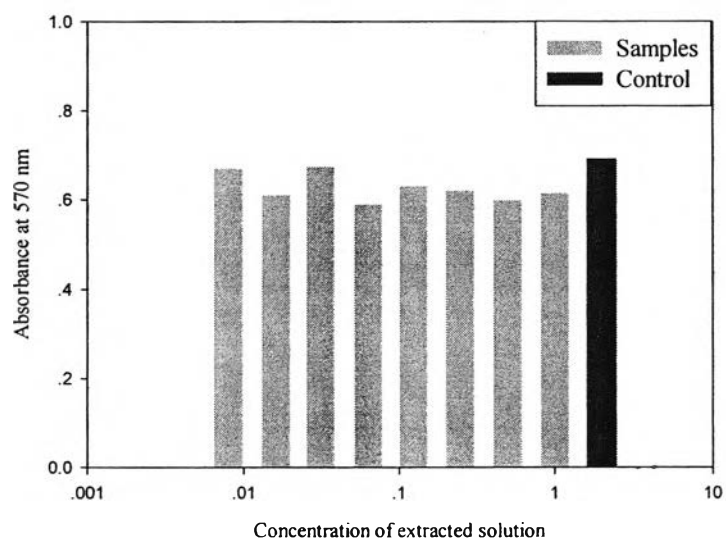


Figure 4.14 The absorbance of MTT result at 570 nm for control and 8 diluted concentration of extracted solution from chitin nanocomposite film.

MTT assay was used to determine the viability of living L929 fibroblasts. The number of viable cells is directly proportional to the absorbance. Fig. 4.14 presents the MTT results by the determination of absorbance at 570 nm. This result shows that the viability of L929 fibroblasts cultured in all of the film extracted solutions was not significantly different from that of the control. The indication suggests that the chitin

nanocomposite film had no effects on the survival of the L929 fibroblasts and it was non-toxic to them.

The MTT assay was also used to investigate the effect of chitin and its derivatives on the growth acceleration of the fibroblast. With the results of Mori, T. *et al.* (1997), the chitin and its derivatives could indirectly accelerate the L929 fibroblast proliferation, but chitin derivatives, which were studied in *in vivo* tests, enhance the rate of L929 fibroblast proliferation. They also found that heparin had some anticoagulant, angiogenic properties and improve mitogenesis. Moreover, heparin was highly effective in accelerating wound healing by forming a complex with chitin and chitosan.

4.11 Cytotoxicity Test by Direct Method (L929 Fibroblast Culture)

Normally, the cell-developing mechanism consists of cell attachment with filopodia, growth of filopodia, cytoplasmic webbing, flattening of the cells and subsequently progressing into their distinguishing characteristics Tanodekaew, S. *et al.* (2004). In this study, the L929 fibroblasts were cultured onto the film surfaces of chitin nanocomposite film, β -chitin film, α -chitin film and chitosan, shown in Fig. 4.15. The time duration used for culturing L929 the fibroblasts was 24, 48 and 72 hours. The cell morphology on all films was found to be significantly different depending on the culture time. At 24 hours, the L929 fibroblast attached, with filopodia, onto the films surface and the L929 morphology was round and contained blebs. In the case of 48 and 72 hours, almost all of the L929 fibroblast morphology was spindle shaped with lamellipodia attaching to the surface. And the L929 became flatter when the culture time was increased. The number of L929 fibroblast on chitin nanocomposite film surface is highest, whereas chitosan show the lowest of cell attachment. When compare the cell attachment with β -chitin film and α -chitin film, the number of L929 fibroblast on α -chitin film surface has much more than β -chitin film surface. This result suggests that chitin has higher biocompatible than chitosan and the chitin nanocomposite is more suitable for cell attachment than the pure chitin. Because the surface of chitin

nanocomposite film is more rough that affect from the chitin whisker filler. Considering to the surface of β -chitin film and α -chitin film, the pure α -chitin film is rougher than that β -chitin film, resulting from the ease of dissolution of β -chitin and the clear solution can obtain, and then the ability of cell attachment on α -chitin film is high.

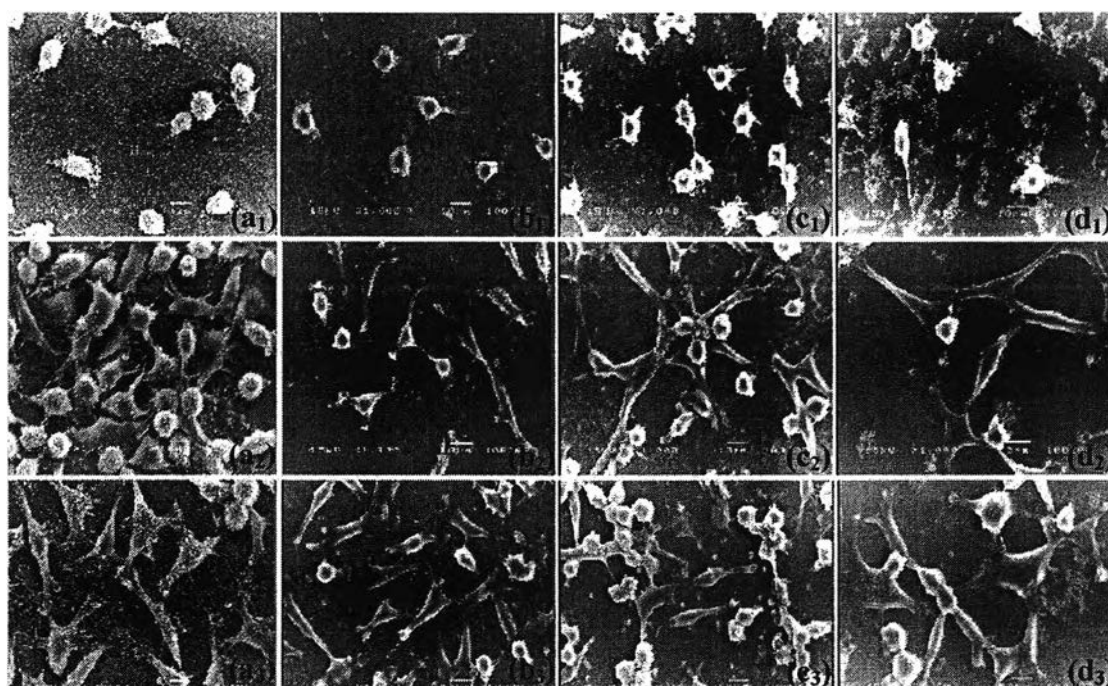


Figure 4.15 SEM images of L929 cultured on (a) chitin nanocomposite, (b) β -chitin, (c) α -chitin and (d) chitosan films for 1, 2 and 3 days.

Both α - and β -chitins are reported to induce the regeneration of epidermal cells during the wound healing process by chitin wound dressing. Chitosan, on the other hand, has been known to accelerate fibroblast formation on the wound (Minagawa, T. *et al.*, 2007, Mori, T. *et al.*, 1997 and Okamoto, Y. *et al.*, 2002), but it is hard to confirm such a clear difference between chitin and chitosan, because chitin molecule carries partly the amino groups among the acetamide groups. In this report, a clear distinction was intended for the inducement of epidermal cell regeneration by chitin, and also to confirm

the dependence of the epidermal cell regeneration on the type of crystalline structure, because preparations of chitin-related membranes with various combinations, such as a heterogeneous mixture or a homogeneous mixture of both types of chitin.